Journal of Southeast University (English Edition) Vol. 27, No. 1, pp. 31 – 35 Mar. 2011 ISSN 1003—7985

Transient characteristics analysis of linear flux-switching permanent magnet machines for precision control

Zhou Shigui[1,2] Yu Haitao[1] Hu Minqiang[1] Huang Lei[1] Yuan Bang[1]

([1] Engineering Research Center for Motion Control of Ministry of Education, Southeast University, Nanjing 210096, China)
([2] School of Electrical Information and Automation, Qufu Normal University, Rizhao 276826, China)

Abstract: A dynamical dq model is proposed for a linear flux-switching permanent magnet (LFSPM) machine which is suitable for high-precision control applications. The operation principle of the prototype machine is analyzed using the finite element method (FEM), and the parameters, such as the back electromotive force (EMF) and the phase flux linkage, are calculated. The calculated and measured results reveal that the back EMF and the flux linkage are essentially sinusoidal, and the variation of the phase flux linkage profile of the LFSPM machine is similar to that of the linear surface permanent magnet (LSPM) machine. Based on this, a dynamical dq model and a simulation control model are proposed. The simulation results are compared with the test results obtained from a DSP-based control platform, which verifies that the model is correct and effective. Moreover, the model can be used for design optimization and control development.

Key words: precision control; flux-switching; permanent magnet machine; dq model; vector control
doi: 10.3969/j.issn.1003 – 7985.2011.01.007

Linear machines have been paid much attention to in the industrial applications for high-precision and high-speed motions during the past decades. They can overcome the limitation in travel distance, accuracy and speed of the traditional actuator, which is composed of a rotary motor and a lead screw. The linear permanent magnet machine (LPMM) is a popular alternative which easily achieves precision control. But it has some shortcomings such as heat, maintenance and manufacture cost problems. The linear switched reluctance motor (LSRM) is also a hotspot in this field due to its simple structure and low cost, but there are many disadvantages, such as low force density, control difficulties and large force ripples. Fortunately, the linear flux-switching permanent magnet (LFSPM) machine combines the advantages and is expected to be a good prospect in this field.

The concept of the rotary flux-switching permanent magnet (FSPM) machine was first proposed in 1955[1]. So far, the design procedure and optimization of the FSPM machine have been investigated[2-6]. Novel linear FSPM machines with varieties of mover slot/stator poles were proposed in Refs. [3-4]. However, the LFSPM machines used for the direct-drive applications of precision machine tools have seldom been investigated. In this paper, an LFSPM machine with armature windings and magnets on the short mover, which combines the merits of both the LPMM machine and the LSRM machine, is analyzed. It is suitable for the direct-drive applications of precision machine tools because of its robustness and controllability. Analysis shows that the phase flux linkage and back EMF of the LFSPM are essentially sinusoidal and the force density is high. Therefore, the proposed LFSPM machine is a competitive candidate for high-precision AC drives[7-9].

1 Construction and Operation Principle

As shown in Fig. 1, the LFSPM machine comprises a mover and a stator. The mover has a plurality of stacks, permanent magnets, and coils, which form a three-phase linear motor, and the stator has a low cost ferromagnetic steel plate which is similar to that of a linear switched reluctance machine. The mover cores are made up of 2 U-shaped cores and 5 E-shaped cores, and each of the E-shaped cores is used to physically couple with two phases to substantially minimize the unexpected cogging force and the force ripple. A permanent magnet is sandwiched between two adjacent cores with alternate magnetic polarities. The mover employs concentrated windings, which consist of two coils in each phase. A suitable design for the LFSPM can achieve optimal electromagnetic coupling between the mover and the stator to obtain high force density [10-11].

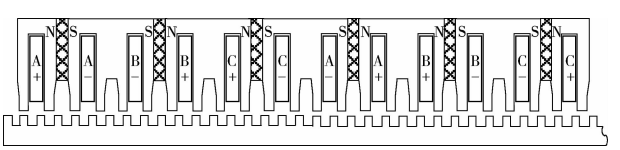

Fig. 1 Schematic of LFSPM machine

Fig. 2 shows the no-load magnetic flux distribution of A1, one of the coils of phase A, in different mover positions.

Assume that the direction of the flux passing through the gap from the mover to the stator is positive and the mover moves to the right. Fig. 2(a) is the initial position where the flux of the A1 coil is the negative maximum. As the mover moves 1/4 stator pole pitch in the right direction, the flux of the coil is zero as shown in Fig. 2(b). Again, the mover moves 1/4 pole pitch, as shown in Fig. 2(c), the flux of the coil at this position is the positive maximum. If the mover moves 1/4 pole pitch further, the mover's position is identical to the initial position. Thus, the machine operates for one whole period.

Received 2010-08-30.
Biographies: Zhou Shigui (1970—), male, graduate; Yu Haitao (corresponding author), male, doctor, professor, htyu@seu.edu.cn.
Foundation item: The National Natural Science Foundation of China (No. 41076054).
Citation: Zhou Shigui, Yu Haitao, Hu Minqiang, et al. Transient characteristics analysis of linear flux-switching permanent magnet machines for precision control[J]. Journal of Southeast University (English Edition), 2011, 27(1): 31 – 35. [doi: 10.3969/j.issn.1003 – 7985.2011.01.007]

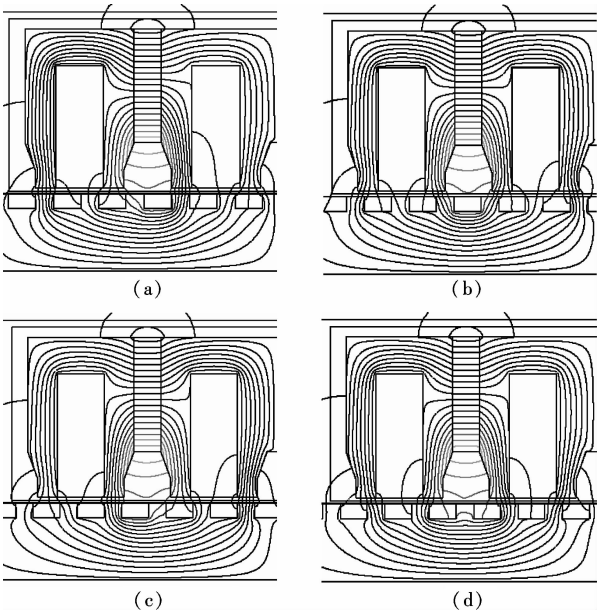

Fig. 2 Flux distribution of LFSPM. (a) 0°; (b) 90°; (c) 180°; (d) 270°

The phase flux linkage waveform of the FSPM machine is bipolar, and the number of pole pairs is equivalent to that of the stator poles. The 3-phase flux-linkage waveform predicted with 2-D finite-element analysis indicates that the waveform is not an ideal sinusoidal waveform and the distortion is mainly induced by end effects. The span of two adjacent phases is equivalent to a $(6-1/3)$ stator pole pitch, i. e., a phase difference of 120° in electrical degree. When the dimensions of the teeth and slots are adjusted properly, the back EMF of the three phases is changed into nearly perfect sinusoidal waveforms after the superposition of the two sets of coils as shown in Fig. 3. The calculated results of the 3-phase back EMF are compared with the measured ones as shown in Fig. 4, which indicates that a good agreement between them is obtained and nearly perfect sinusoidal waveforms are achieved.

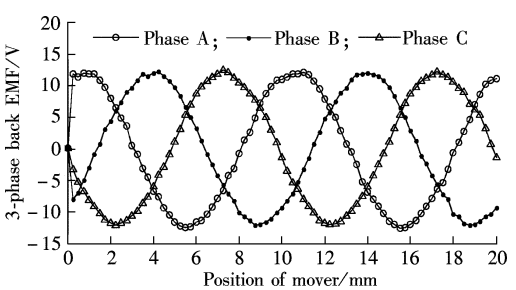

Fig. 3 Simulation of 3-phase back EMF at 0. 5 m/s

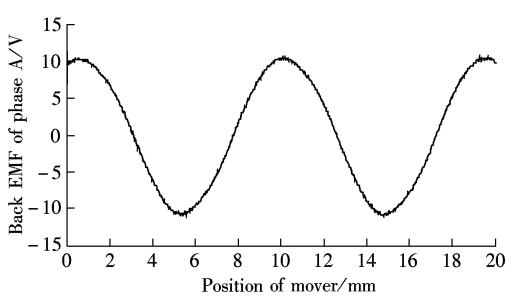

Fig. 4 Measured phase A back EMF at 0. 5 m/s

2 Modeling

For an LFSPM machine, the permanent magnet field is changed twice while the mover moves a distance of one stator pole pitch, that is, 360° in electrical degree. The dq axis of the permanent magnet field is distinguished using the FEM as follows: The d-axis is located on the stator position where the permanent magnet (PM) flux linkage of phase A is maximum (as shown in Fig. 2 (a)) and the q-axis advances d-axis by 90° in electrical degree (a quarter of one stator pole pitch), as shown in Fig. 5(a). The d-axis component of the synthesis magnetic-motive force(MMF) produced by a 3-phase current can be aligned with the direction of the PM field by controlling the armature current, and the MMF q-axis component is perpendicular to the d-axis component. Besides, for the optimal force related to the armature current, we set $i_d = 0$, and i_q to be equivalent to the armature current. Therefore, the armature current can be changed to directly control the amplitude of the output force. This control strategy is called as the $i_d = 0$ vector control method based on the PM field orientation. The above analysis shows that the LFSPM electromagnetic characteristic is equivalent to that of sinusoidal surface magnet machines (SPM), and the $i_d = 0$ vector control strategy is equivalent to that of SPM based on the rotor field orientation. The comparisons of the topologies and the 3-phase flux waveforms of the two machines are shown in Fig. 5.

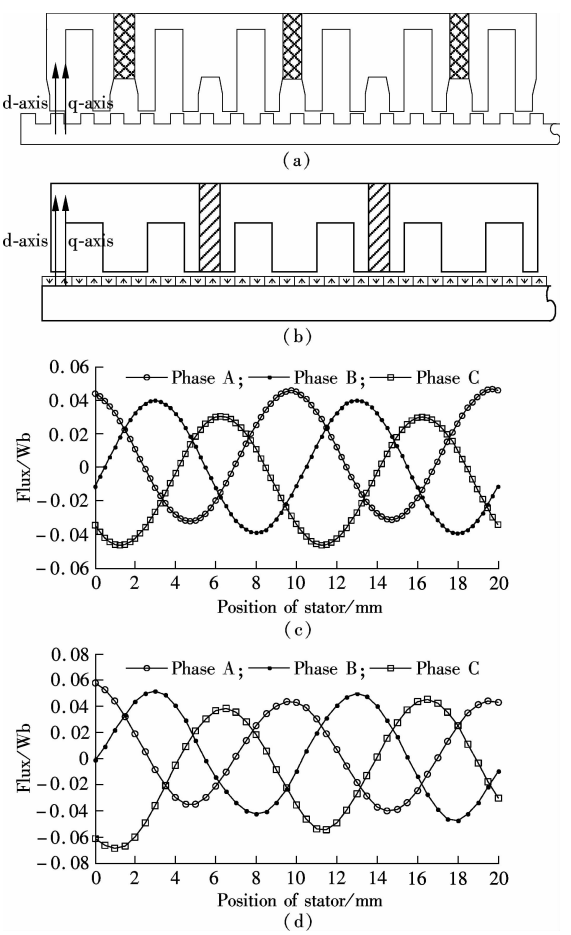

Fig. 5 Comparison of LFSPM machine and LSPM machine. (a) Topology of LFSPM machine; (b) Topology of LSPM machine; (c) PM flux linkage of LFSPM machine; (d) PM flux of LSPM machine

Thus, the FSPM machine can be modeled as follows. The d-axis and q-axis flux linkage equations and the voltage equation are derived as

$$\left.\begin{aligned}\psi_{\mathrm{d}} &= \psi_{\mathrm{m}} + L_{\mathrm{d}} i_{\mathrm{d}} \\ \psi_{\mathrm{q}} &= L_{\mathrm{q}} i_{\mathrm{q}}\end{aligned}\right\} \tag{1}$$

$$\left.\begin{aligned}\frac{\mathrm{d}\psi_{\mathrm{d}}}{\mathrm{d}t} &= u_{\mathrm{d}} + \frac{2\pi}{\tau} v_{\mathrm{e}} \psi_{\mathrm{q}} - R_{\mathrm{s}} i_{\mathrm{d}} \\ \frac{\mathrm{d}\psi_{\mathrm{q}}}{\mathrm{d}t} &= u_{\mathrm{q}} - \frac{2\pi}{\tau} v_{\mathrm{e}} \psi_{\mathrm{d}} - R_{\mathrm{s}} i_{\mathrm{q}}\end{aligned}\right\} \tag{2}$$

The thrust force equation is

$$F_{\mathrm{e}} = \frac{3}{2} \frac{2\pi}{\tau} [\psi_{\mathrm{m}} i_{\mathrm{q}} + (L_{\mathrm{d}} - L_{\mathrm{q}}) i_{\mathrm{d}} i_{\mathrm{q}}] \tag{3}$$

where τ is the stator pole pitch; L_{d} and L_{q} are the d-axis and q-axis inductances of the FSPM machine; ψ_{m} is the flux linkage of PM.

The parameters ψ_{m}, L_{d} and L_{q} are determined by FEM and tests. ψ_{m} can be easily calculated, and the calculation of L_{d} and L_{q} is described in the following sections[12-13].

According to the previous method of determining the direction of the PM field, the d-axis and q-axis of the proposed LFSPM machine are determined. Assume that the 3-phase coils are powered with current sources according to 3-phase currents $i_{\mathrm{B}} = i_{\mathrm{C}} = -0.5 i_{\mathrm{A}}$, then the inductance parameters L_{d} and L_{q} can be calculated using Maxwell 2D when the mover is fixed on the positions of the d-axis and the q-axis, respectively. Moreover, the relationship between the inductances of the dq-axis and the armature current can be analyzed while the current is changed.

Half of the prototyped machine is used in simulation because of the symmetry. The number of A-phase turns is half those of the actual number of turns. The calculated flux linkage is also half that of the actual one. The calculation equations of inductance on the d-axis and the q-axis are obtained as follows:

$$L_{\mathrm{d}} = \frac{2\psi_{\mathrm{A}} - \psi_{\mathrm{m}}}{i_{\mathrm{AT}}/N} \tag{4}$$

$$L_{\mathrm{q}} = \frac{2\psi_{\mathrm{A}}}{i_{\mathrm{AT}}/N} \tag{5}$$

where i_{AT} is MMF generated by i_{A}; N denotes the turns of coils; and ψ_{A} is the flux linkage in phase A where the mover is located on the position of the d-axis or the q-axis. The predicted profiles of L_{d} and L_{q} versus the armature current are shown in Fig. 6.

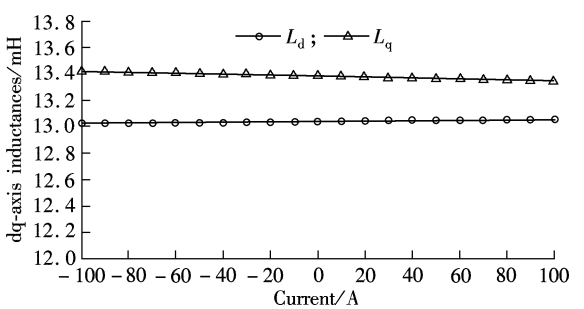

Fig. 6 Predicted d-axis and q-axis inductances

3 Simulation and Test

The simulation model of the proposed control system is presented according to the forgoing control method. The mathematical model of the LFSPM machine uses the model proposed in section 2 and the block diagram of the control system for the LFSPM motor is presented in Fig. 7. The feedback signal which can determine the position of the PM field and the speed of the mover is the displacement of the mover. The position signal θ directly generates unit vector signals ($\cos\theta_{\mathrm{e}}$ and $\sin\theta_{\mathrm{e}}$). The control system consists of a velocity loop and a current loop. The velocity loop generates the reference current i_{q}, but i_{d} equals zero. The reference of 3-phase current is obtained and transformed by 2/3 coordinate transformation. The reference current is compared with the 3-phase measured current through the hysteresis; thus, the actual output current wave is forced to track the sine reference wave within the hysteresis band. Finally, the LFSPM machine can stably operate at the reference speed[14-15].

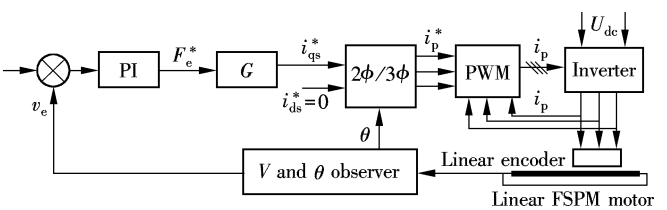

Fig. 7 Overall control block diagram for the LFSPM motor

The test platform includes a controller and a prototyped LFSPM machine. The control method is successfully implemented on the control platform based on TMS320F2812 DSP. A Renishaw optical linear encoder is used for the collection of the velocity and the position of the mover. LEM LTSR 6-NP current transducers are used to measure the phase currents, and intelligent power modules (IPMs) PM75CSD120 are also installed for power output [15-16]. The calculated and measured plots of the A-phase current when the velocity of the mover changes from 0.1 to 0.2 m/s are shown in Fig. 8(a) and Fig. 9(a). Fig. 8(b) and Fig. 9(b) show the plots of predicted and measured current waveforms when the load is changed from 10 to 30 N. As can be seen from the profiles, the predicted and measured waveforms are both in nearly perfect sinusoidal distributions, and good agreements are achieved between them. It is demonstrated that the motor model is correct and effective, and it can be used for performance evaluation and simulation analysis.

4 Conclusion

LFSPM machines have a doubly salient mover and stator topology, with concentrated winding and permanent magnet in the short mover. Unlike the LSRM, the back EMF of the LFSPM machine is essentially sinusoidal, which enables the motor to be easily controlled. The long stator is made of silicon steel; therefore, the heat, maintenance and manufacture cost problems are eliminated. The pole pitch of the LFSPM machine can be changed easily by selecting stators with different pole numbers, which can affect the motor synchronous speed accordingly. So the LFSPM machine has

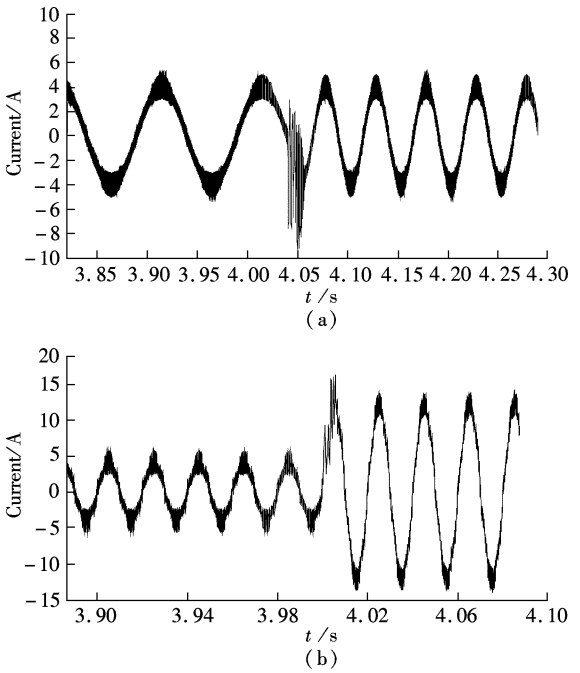

Fig. 8 Simulated current waveforms. (a) Current waveform of velocity changes; (b) Current waveform of load changes

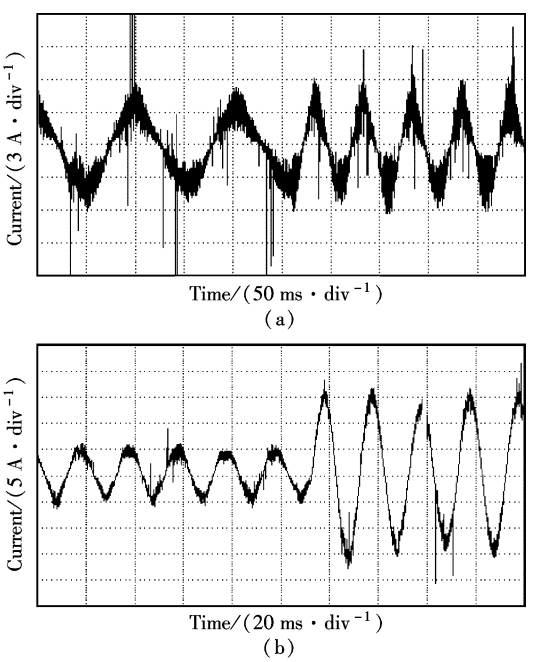

Fig. 9 Measured current waveform. (a) Current waveform of velocity changes; (b) Current waveform of load changes

great potential for the fields of high-precision and high-speed motion control. This paper proposes a transient model for the LFSPM machine and provides a magnetic field orientation method for finding dq axis inductance. Simulations and tests of the control system validate that the proposed model and the theory analysis are correct and that the LFSPM machine is applicable to high-precision AC servo control drives.

References

[1] Rauch S E, Johnson L J. Design principles of flux-switching alternators [J]. *Transactions of the American Institute of Electrical Engineers*, 1955, **74**(3): 1261 − 1268.

[2] Zhu Z Q, Pang Y, Howe D. Analysis of electromagnetic performance of flux-switching permanent magnet machines by non-linear adaptive lumped parameter magnetic circuit model [J]. *IEEE Transactions on Magnetics*, 2005, **41**(11): 4277 − 4287.

[3] Zhu Z Q, Chen X, Chen J T, et al. Novel linear flux-switching permanent magnet machines [C]//*International Conference on Electrical Machines and Systems*. Wuhan, China, 2008: 2948 − 2953.

[4] Jin Mengjia, Wang Canfei, Shen Jianxin, et al. A modular permanent-magnet flux-switching linear machine with fault-tolerant capability [J]. *IEEE Transactions on Magnetics*, 2009, **45**(8): 3179 − 3186.

[5] Zhu Z Q, Chen J T. Advanced flux-switching permanent magnet brushless machines [J]. *IEEE Transactions on Magnetics*, 2010, **46**(6): 1447 − 1453.

[6] Zhu Z Q, Chen J T, Pang Y, et al. Analysis of a novel multi-tooth flux-switching PM brushless AC Machine for high torque direct-drive applications [J]. *IEEE Transactions on Magnetics*, 2008, **44**(11): 4313 − 4316.

[7] Hua Wei, Cheng Ming, Lu Wei, et al. A new stator-flux orientation strategy for flux-switching permanent magnet motor based on current-hysteresis control [J]. *Journal of Applied Physics*, 2009, **105**: 07F112.

[8] Hua Wei, Cheng Ming. Inductance characteristics of 3-phase flux-switching permanent magnet machine with doubly-salient structure [J]. *Transactions of China Electrotechnical Society*, 2007, **22**(11): 21 − 28.

[9] Jia Hongyun, Cheng Ming, Hua Wei, et al. A new stator-flux orientation strategy for flux-switching permanent motor drive based on voltage space-vector[C]//*International Conference on Electrical Machines and Systems*. Wuhan, China, 2008: 2032 − 3036.

[10] Chen J T, Zhu Z Q, Howe D. Stator and rotor pole combinations for multi-tooth flux-switching permanent-magnet brushless AC machines [J]. *IEEE Transactions on Magnetics*, 2008, **44**(12): 4659 − 4667.

[11] Chen J T, Zhu Z Q. Winding configurations and optimal stator and rotor pole combination of flux-switching PM brushless AC machines [J]. *IEEE Transactions on Industry Applications*, 2010, **25**(2): 293 − 302.

[12] Cheng Shukang, Yu Yanjun, Chai Feng, et al. Analysis of the inductances of interior permanent magnet synchronous motor[J]. *Proceedings of the CSEE*, 2009, **29**(18): 94 − 99.

[13] Rahman K M, Silva H. Identification of machine parameters of a synchronous motor [J]. *IEEE Transactions on Industry Applications*, 2005, **42**(2): 557 − 565.

[14] Miller T J E, Popescu M, Cossar C, et al. Performance estimation of interior permanent-magnet brushless motors using the voltage-driven flux-MMF diagram [J]. *IEEE Transactions on Magnetics*, 2006, **42**(7): 1867 − 1872.

[15] Bose B K. *Modern power electronics and AC drives*[M]. New Jersey: Prentice Hall, 2002: 465 − 482.

[16] Chau K T, Li Y B, Jiang J Z, et al. Design and control of a PM brushless hybrid generator for wind power application [J]. *IEEE Transactions on Magnetics*, 2006, **42**(10): 3497 − 3499.

用于精密控制的直线磁通切换永磁电动机的暂态性能分析

周士贵[1,2] 余海涛[1] 胡敏强[1] 黄 磊[1] 袁 榜[1]

([1] 东南大学伺服控制技术教育部工程研究中心,南京 210096)

([2] 曲阜师范大学电气信息与自动化学院,日照 276826)

摘要:提出了一种适用于精密控制的新型直线磁通切换永磁(LFSPM)电机的动态 dq 数学模型. 通过采用有限元法对 LFSPM 原型机进行数值仿真,分析该电机的运行原理并计算其反电动势、磁链等电磁参量. 仿真和测量表明,该电机的反电动势和磁链均按正弦规律变化,并且在运行时具有与直线表面永磁电机(LSPM)相似的磁链变化规律. 在此基础上,提出了该电机的动态 dq 数学模型,建立了电机的控制仿真模型. 仿真结果与在基于 DSP 控制实验平台上测得的结果进行比较,验证了所建数学模型的正确性和有效性. 该模型可用于该类电机的设计优化和控制性能方面的研究.

关键词:精密控制;磁通切换;永磁电动机;dq 模型;矢量控制

中图分类号:TM351